Highly Efficient Blue Organic Light-Emitting Device Based on a Nondoped Electroluminescent Material

Qing-Xiao Tong,*[,†,‡] Shiu-Lun Lai,[‡,||] Mei-Yee Chan,[‡,||] Ye-Chun Zhou,[‡,||] Hoi-Lun Kwong,[§] Chun-Sing Lee,[‡,||] and Shuit-Tong Lee*[,‡,||]

Department of Chemistry, Shantou University, Guangdong 515063 China, and Center of Super-Diamond and Advanced Films (COSDAF), Department of Biology and Chemistry, and Department of Physics and Materials Science, City University of Hong Kong, Hong Kong SAR, China

Received May 20, 2008
Revised Manuscript Received September 4, 2008

Since the first high-efficiency small-molecule organic light-emitting device (OLED) was reported,[1] intense research effort has been focused in developing high-performance emitting materials to realize flat panel displays as well as solid-state lightings.[2−4] In particular, the development of highly efficient and stable blue-emitting material draws special attention. Blue-emitting material not only is the major constituent for red-green-blue full color displays, but also the key emitting element for generating white light in combination with complementary yellow color. Due to its intrinsic larger bandgap, the blue emitter also can serve as a host for a variety of dopant emitters. Since the first report of blue OLED by Adachi et al.,[5] extensive studies on the design and synthesis of blue light-emitting materials have been demonstrated. One of the classical blue host emitters in OLED is 9,10-di-(2-naphthyl) anthracene (ADN).[6] It exhibits a high electroluminescence (EL) efficiency (∼1.9 cd/A) and blue emission with the Commission Internationale d'Eclairage (CIE) coordinates of (0.20,0.26). However, the ADN molecules are easily crystallized under a prolonged electrical stress or under an elevated temperature, leading to reduced device lifetime. More recently, Lee et al.[7] has modified the ADN structure by introducing methyl group at the C-2 position of ADN, namely 2-methyl-9,10-di(2-naphthyl) anthracene (MADN), in order to enhance its morphological stability and color purity. The nondoped MADN-based OLED demonstrates the efficiencies of 1.4 cd/A and 0.7 lm/W, and deep blue emission of (0.15,0.10). Device efficiency can be further improved by doping with 3% sky-blue fluorescent dopant material, e.g., *p*-bis(*p*-*N*,*N*-diphenyl-aminostyryl) benzene (DSA-Ph), thereby achieving high current and power efficiencies of 9.7 cd/A and 5.5 lm/W, respectively.

Understandably, the success of this doping method relies on the precise control of dopant concentration (usually <5%).[7,8] Undoubtedly, it imposes severe challenges on the prospective manufacturing process and thus increases the manufacturing cost. In addition, phase separation in a guest−host system is also a potential problem,[9−11] because recent work has proven that phase separation upon heating is an important cause for performance degradation in some guest−host system-based devices. Although host and guest molecules are initially homogeneously mixed, guest molecules frequently aggregate leading to phase separation during operation and/or upon heating. Phase separation increases the host−guest distance beyond the available distance R (1−10 nm) or capture radius of a guest molecule for efficient host−guest energy transfer, thus rendering energy transfer ineffective.[12] This phenomenon can further reduce device lifetime, especially under high-temperature operation. In view of these shortcomings, considerable efforts have recently been devoted to the synthesis of high-efficiency nondoped emitters.[13−22]

Here, we report a highly efficient blue OLED based on a newly synthesized material 3,6-di[8-(7,10-diphenylfluoranthenyl)]-9-[4′-tert-butylphenyl]carbazole (DDPFTBC). The DDPFTBC-based nondoped device demonstrated a stable blue emission with the CIE coordinates of (0.18, 0.36), high current and power efficiencies of 8.7 cd/A and 9.1 lm/W, respectively, comparably higher than those of any nondoped fluorescence blue OLEDs ever reported.

* Corresponding authors. E-mail: qxtong@gmail.com (Q.-X.T.); apannale@cityu.edu.hk (S.-T.L.).
† Shantou University.
‡ Center of Super-Diamond and Advanced Films, City University of Hong Kong.
§ Department of Biology and Chemistry, City University of Hong Kong.
|| Department of Physics and Materials Science, City University of Hong Kong.

(1) Tang, C. W.; VanSlyke, S. A. *Appl. Phys. Lett.* **1987**, *51*, 913.
(2) Chen, C. H.; Shi, J. *Coord. Chem. Rev.* **1998**, *171*, 161.
(3) Friend, R. H.; Gymer, R. W.; Holmes, A. B.; Burroughes, J. H.; Marks, R. N.; Taliani, C.; Bradley, D. D. C.; Santos, D. A. D.; Brédas, J. L.; Lögdlund, M.; Salaneck, W. R. *Nature.* **1999**, *397*, 121.
(4) Kraft, A.; Grimsdale, A. C.; Holmes, A. B. *Angew. Chem., Int. Ed.* **1998**, *37*, 402.
(5) Adachi, C.; Tsutsui, T.; Saito, S. *Appl. Phys. Lett.* **1990**, *56*, 799.
(6) Shi, J.; Tang, C. W. *Appl. Phys. Lett.* **2002**, *80*, 3201.
(7) Lee, M. T.; Chen, H. H.; Liao, C. H.; Tsai, C. H.; Chen, C. H. *Appl. Phys. Lett.* **2004**, *85*, 3301.
(8) Tang, C. W.; VanSlyke, S. A.; Chen, C. H. *J. Appl. Phys.* **1989**, *65*, 3610.
(9) Zhong, G. Y.; Xu, Z.; Zhang, S. T.; Zhan, Y. Q.; Wang, X. J.; Xiong, Z. H.; Shi, H. Z.; Ding, X. M.; Huang, W; Hou, X. Y. *Appl. Phys. Lett.* **2002**, *81*, 1122.
(10) Chang, S. C.; He, G.; Chen, F. C.; Guo, T. F.; Yang, Y. *Appl. Phys. Lett.* **2001**, *79*, 2088.
(11) Gong, J. R.; Wan, L. J.; Lei, S. B.; Bai, C. L.; Zhang, X. H.; Lee, S. T. *J. Phys. Chem. B* **2005**, *109*, 1675.
(12) Baldo, M. A.; O'Brien, D. F.; You, Y.; Shoustikov, A.; Sibley, S.; Thompson, M. E.; Forrest, S. R. *Nature* **1998**, *395*, 151.
(13) Robinson, M. R.; Bazan, G. C.; O'Regan, M. B. *Chem. Commun. (Cambridge)* **2000**, 1645.
(14) Murata, H.; Kafafi, Z. H.; Uchida, M. *Appl. Phys. Lett.* **2002**, *80*, 189.
(15) Lee, C. L.; Kang, N. G.; Cho, Y. S.; Lee, J. S.; Kim, J. J. *Opt. Mater.* **2002**, *21*, 119.
(16) Xin, H.; Li, F. Y.; Guan, M.; Huang, C. H.; Sun, M.; Wang, K. Z.; Zhang, Y. A.; Jin, L. P. *J. Appl. Phys.* **2003**, *94*, 4729.
(17) Lo, S. C.; Namdas, E. B.; Burn, P. L.; Samuel, I. D. W. *Macromolecules* **2003**, *36*, 9721.
(18) Wong, W. Y.; He, Z.; So, S. K.; Tong, K. L.; Lin, Z. *Organometallics* **2005**, *24*, 4079.
(19) Li, Y.; Rizzo, A.; Salerno, M.; Mazzeo, M.; Huo, C.; Wang, Y.; Li, K.; Cingolani, R.; Giglib, G. *Appl. Phys. Lett.* **2006**, *89*, 061125.
(20) Tong, Q. X.; Lai, S. L.; Chan, M. Y.; Tang, J. X.; Kwong, H. L.; Lee, C. S.; Lee, S. T. *Appl. Phys. Lett.* **2007**, *91*, 023503.
(21) Tong, Q. X.; Lai, S. L.; Chan, M. Y.; Tang, J. X.; Kwong, H. L.; Lee, C. S.; Lee, S. T. *Appl. Phys. Lett.* **2007**, *91*, 153504.
(22) Tong, Q. X.; Lai, S. L.; Chan, M. Y.; Zhou, Y. C.; Kwong, H. L.; Lee, C. S.; Lee, S. T. *Chem. Phys. Lett.* **2008**, *455*, 79.

10.1021/cm801304t CCC: $40.75
Published on Web 09/24/2008

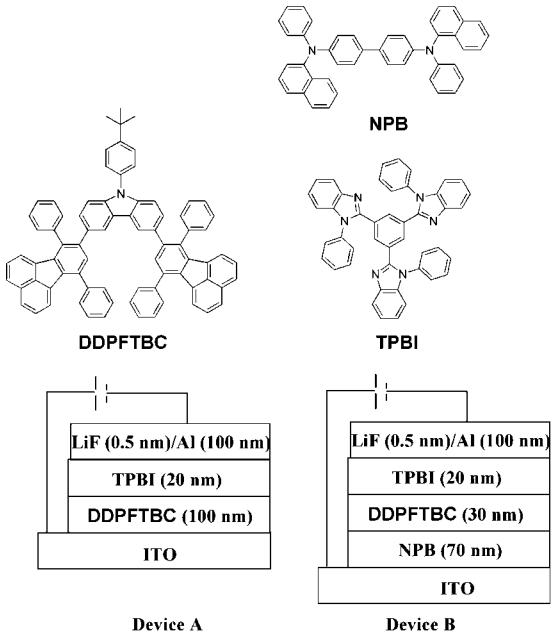

Figure 1. Chemical structures of the employed materials and OLED architectures.

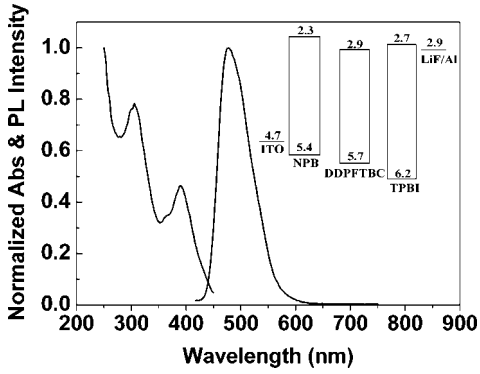

Figure 2. Absorption and photoluminescence spectra of DDPFTBC film on a quartz substrate. Inset: the energy level diagram for the device.

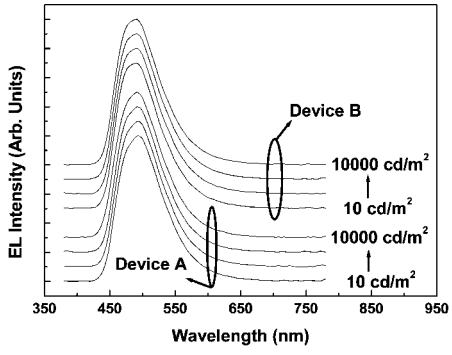

Figure 3. Electroluminescence spectra of devices A and device B viewed in the normal direction at the luminance of 10, 100, 1000, and 10000 cd/m^2, respectively.

Figure 1 shows the chemical structures of DDPFTBC, NPB, and TPBI, along with the device architectures. The as-synthesized product DDPFTBC was confirmed by ^{1}H-nuclear magnetic resonance, elemental analysis, and mass spectrometry. Figure 2 depicts the absorption and PL spectra of a DDPFTBC thin film deposited on a quartz substrate, showing a strong blue emission with peak at 478 nm. An

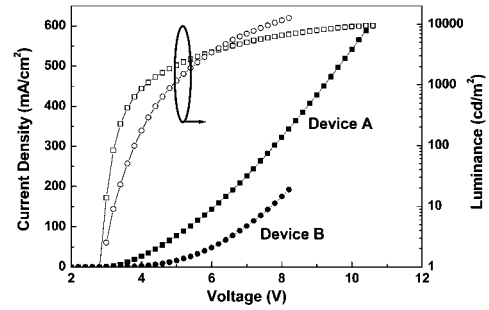

Figure 4. Current density−voltage−luminance characteristics of device A (□, ■) and device B (○, ●).

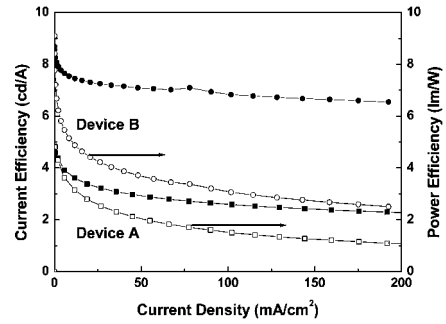

Figure 5. Current efficiency−current density−power efficiency characteristics of device A (□, ■) and device B (○, ●).

inset in Figure 2 illustrates the energy level diagram for the OLED. From the UPS analysis, the HOMO of DDPFTBC was determined at 5.7 eV. Subtracting the optical bandgap of 2.8 eV (i.e., determined by the cutoff of optical absorption spectrum) from the HOMO level, the LUMO of DDPFTBC was estimated to be 2.9 eV.

Figure 3 depicts the EL spectra for devices A and B viewed in the normal direction at the luminance of 10, 100, 1000, and 10000 cd/m^2, respectively. Remarkably, blue light emission was obtained from both devices A and B with a dominating peak at 492 nm with a full spectral width at half-maximum (fwhm) of 79 ± 1.0 nm. It is worth noting that both devices exhibit nearly identical CIE coordinates of (0.18, 0.37 ± 0.01). In addition, the EL spectra for both devices are almost independent of the driving voltages, with the fwhm remained unchanged over a wide luminance range of 10−10000 cd/m^2. It suggests that the hole and electron recombination is well confined within the DDPFTBC layer.It is a common phenomenon that the EL spectrum of blue-emitting OLEDs shifts under different electric fields. This is mainly attributed to the difference in the charge carrier mobility in the employed organic layers, resulting in the shift of the emission region. However, it is not the case for the present DDPFTBC-based devices (i.e., the CIE coordinates remain constant over a wide luminance range), which is of particular importance for the commercial full-color applications. It should be mentioned that our recent study[20] on the use of another new blue-emitter 4,4′,4″-trispyrenylphenylamine (TPyPA) showed exciplex formation at the TPyPA/TPBI interface, resulting in an additional emission peak at 570 nm. Significantly, exciplex formation does not occur in the present case, which may be attributed to a weaker electron-donating property of DDPFTBC as compared to the TPyPA.

Table 1. Performance Parameters of the Present and Several Recently Reported Blue OLEDs

light-emitter[a]	turn-on voltage (V)	voltage @ 20 mA/cm^2 (V)	maximal current efficiency (cd/A)	maximal power efficiency (lm/W)	emission peaks (nm)	CIE$_{x,y}$ coordinates (x,y)	ref
DDPFTBC	2.8	5.2	8.7	9.1	492	0.18,0.36	This work
BUBD-1:MADN		6.7	13.2	6.1	466 500	0.16,0.30	23
DPF	5.2		5.3	3.0	469	0.16,0.22	24
DSA-Ph:MADN		5.7	9.7	5.5	464 490	0.16,0.32	7
MADN		6.2	1.4	0.7	452	0.15,0.10	
TBP:ADN		9.1	3.4	1.8	465 496	0.15,0.23	6

[a] BUBD-1, −; MADN, 2-methyl-9,10-di(2-naphthyl) anthracene; DPF, 2,7-dipyrene-9,9′-dimethyl fluorene; DSA-Ph, *p*-bis(p-N,N-diphenyl-amino-styryl) benzene; TBP, 2,5,8,11-tetra-t-butylperylene; ADN, 9,10-di-(2-naphthyl) anthracene.

Figure 4 shows the J−V−L characteristics of the devices. At the same driving voltage (<6 V), device A exhibits a higher current density and a higher luminance than device B, although the turn-on voltage (defined as voltage required to obtain a luminance of 1 cd/m^2) of both devices are the same (2.8 V). For instance, at the operating voltage of 5 V, the current density and the luminance for device A are 77.6 mA/cm^2 and 2100 cd/m^2, respectively, while those for device B are only 15.9 mA/cm^2 and 1170 cd/m^2. It is surprising that the driving voltage for device A is much lower than that for device B, since NPB can act as a stepping-stone to facilitate hole injection at the ITO/DDPFTBC contacts. The reason for these discrepancies may be attributed to different carrier mobilities in the organic layers. The present results appear to suggest that the hole mobility in DDPFTBC is comparatively higher than that in NPB, thus resulting in a lower driving voltage.

On the other hand, the incorporation of NPB can significantly improve device efficiencies. As depicted in Figure 5, the maximum current and power efficiencies of device A are 4.6 cd/A (η_{EQE} = 1.97%) and 4.8 lm/W, respectively, whereas those of device B are 8.7 cd/A (η_{EQE} = 3.93%) and 9.1 lm/W, respectively. The performance improvement may be attributed to a better balance of hole and electron currents within the DDPFTBC layer, due to the lower hole mobility in NPB than that in DDPFTBC, consistent with the device characteristics. The efficiencies of the present DDPFTBC-based devices are higher than those of the recently reported blue OLEDs with nondoped and doped light-emitters.[6,7,23,24] Table 1 compares the device performance of the present DDPFTBC-based device with those of the recently reported ones. Remarkably, the DDPFTBC-based device has comparable or better performance than any of the blue OLEDs, in terms of efficiencies and turn-on voltages. More importantly, the present device exhibits the highest power efficiency (9.1 lm/W) among the best ever reported in the literatures, although its color purity has room for improvement. Although we have not measured the device stability, we noticed that the DDPFTBC-based device is quite stable, and its current efficiency remains a high value even after several days of storage. These excellent device performances illustrate DDPFTBC is the suitable candidate for commercial applications.

In summary, we have fabricated a highly efficient nondoped blue OLED by using a novel EL material DDPFTBC. The device with a simple structure of ITO/NPB/ DDPFTBC/ TPBI/LiF/Al demonstrated a high current efficiency of 8.7 cd/A, and a high power efficiency of 9.1 lm/W. It shows stable blue emission with the CIE coordinates of (0.18, 0.36), with the CIE coordinates and the fwhm remaining unchanged over a wide luminance range from 10 to 10000 cd/m^2.

Experimental Section

Patterned indium−tin oxide (ITO)-coated glass substrates with a sheet resistance of 30 Ω per square were cleaned sequentially with isopropyl alcohol, Decon 90, and deionized water, then dried in an oven, and finally treated in an ultraviolet-ozone chamber. The ITO substrates were then transferred into a deposition chamber which had a base pressure of 10^{-6} mbar. Two devices with structures of ITO/DDPFTBC (100 nm)/TPBI (20 nm)/LiF (0.5 nm)/Al (100 nm) (device A) and ITO/NPB (70 nm)/DDPFTBC (30 nm)/TPBI (20 nm)/LiF (0.5 nm)/Al (100 nm) (device B) were fabricated, in which *N*,*N*′-bis(1-naphthyl)-*N*,*N*′-diphenyl-1,1′-biphenyl-4,4′-diamine (NPB) and 1,3,5-tris(*N*-phenylbenzimidazol-2-yl) benzene (TPBI) served as hole-transporting and electron-transporting materials, respectively. For device A, DDPFTBC was employed as both the light-emitting and hole-transporting materials. Finally, a 0.5 nm thick LiF and a 100 nm thick Al cathode were deposited by thermal evaporation through a shadow mask giving an active device area of 0.1 cm^2. Deposition rates were monitored with a quartz oscillation crystal and controlled at 1−2 Å/s for both organic and metal layers. EL and current density−voltage−luminance (J−V−L) characteristics of OLEDs were measured with a programmable Keithley model 237 power source and a Spectrascan PR 650 photometer under ambient air conditions. Absorption and photoluminescence (PL) spectra of DDPFTBC were measured with a Perkin-Elmer Lambda UV−vis spectrometer. The highest occupied molecular orbital (HOMO) level of DDPFTBC was measured with ultraviolet photoelectron spectroscopy (UPS) in a VG ESCALAB 220i-XL surface analysis system. From the HOMO value the lowest unoccupied molecular orbital (LUMO) level of DDPFTBC was estimated using the optical band gap determined from the absorption spectrum of its solid thin film.

Acknowledgment. This work was financially supported by the Innovation and Technology Commission and the National Science Foundation of China (20502013).

CM801304T

(23) Lin, M. F.; Wang, L.; Wong, W. K.; Cheah, K. W.; Tam, H. L.; Lee, M. T.; Chen, C. H. *Appl. Phys. Lett.* **2006**, *89*, 121913.
(24) Tao, S. L.; Peng, Z. K.; Zhang, X. H.; Wang, P. F.; Lee, C. S.; Lee, S. T. *Adv. Funct. Mater.* **2005**, *15*, 1716.